Vol. 85, No. 17

Binding of Avian Coronavirus Spike Proteins to Host Factors Reflects Virus Tropism and Pathogenicity[▽][†]

I. N. Ambepitiya Wickramasinghe,[1] R. P. de Vries,[2] A. Gröne,[1]
C. A. M. de Haan,[2] and M. H. Verheije[1]*

*Pathology Division, Department of Pathobiology,[1] and Virology Division, Department of Infectious Diseases & Immunology,[2]
Faculty of Veterinary Medicine, Utrecht University, Utrecht, The Netherlands*

The binding of viruses to host cells is the first step in determining tropism and pathogenicity. While avian infectious bronchitis coronavirus (IBV) infection and avian influenza A virus (IAV) infection both depend on α2,3-linked sialic acids, the host tropism of IBV is restricted compared to that of IAV. Here we investigated whether the interaction between the viral attachment proteins and the host could explain these differences by using recombinant spike domains (S1) of IBV strains with different pathogenicities, as well as the hemagglutinin (HA) protein of IAV H5N1. Protein histochemistry showed that S1 of IBV strain M41 and HA of IAV subtype H5N1 displayed sialic acid-dependent binding to chicken respiratory tract tissue. However, while HA bound with high avidity to a broad range of α2,3-linked sialylated glycans, M41 S1 recognized only one particular α2,3-linked disialoside in a glycan array. When comparing the binding of recombinant IBV S1 proteins derived from IBV strains with known differences in tissue tropism and pathogenicity, we observed that while M41 S1 displayed binding to cilia and goblet cells of the chicken respiratory tract, S1 derived from the vaccine strain H120 or the nonvirulent Beaudette strain had reduced or no binding to chicken tissues, respectively, in agreement with the reduced abilities of these viruses to replicate in vivo. While the S1 protein derived from the nephropathogenic IBV strain B1648 also hardly displayed binding to respiratory tract cells, distinct binding to kidney cells was observed, but only after the removal of sialic acid from S1. In conclusion, our data demonstrate that the attachment patterns of the IBV S proteins correlate with the tropisms and pathogenicities of the corresponding viruses.

The binding of a virus to the host cell is the first step in determining tissue and host specificity and, ultimately, pathogenicity. While some viruses, such as influenza A virus (IAV), bind to relatively abundant and universal host factors and may therefore infect various host species, other viruses have a more restricted repertoire of susceptible hosts, limited by their requirement for specific virus receptors on host cells. In general, coronaviruses, which cause respiratory and/or intestinal infections in either avian or mammalian species, are examples of viruses with a narrow host tropism.

Coronaviruses are enveloped, positive-strand RNA viruses of both human and veterinary importance. Infectious bronchitis virus (IBV) is the prototype avian coronavirus, belonging to the genus *Gammacoronavirus*. IBV infections are restricted to domestic fowl (predominantly chickens [*Gallus gallus*]), causing a highly contagious respiratory disease with huge economic impact. Many IBV genotypes and serotypes, which differ extensively in their pathogenicities for poultry, are circulating worldwide (reviewed in reference 15). The initial target of IBV is the epithelial surface of the respiratory tract, but IBV also infects several nonrespiratory tissues, such as the gastrointestinal tract, the oviduct, and the kidney. Infection of the enteric tissues is usually not associated with clinical signs, while repli-

cation in the kidney might cause nephropathogenicity depending on the IBV strain (reviewed in reference 15). Thus, while the IBV host tropism is restricted to chickens, the cell and tissue tropism in chickens differs greatly between different IBV strains.

The coronaviral envelope contains the major attachment spike (S) protein, the membrane (M) protein, and the minor envelope (E) protein (reviewed in reference 60). The spikes, consisting of trimers of S proteins (21), are required for attachment to cells and subsequent fusion of the viral and cellular membranes. The S protein is thus largely responsible for cell and host tropism. In agreement with this, it has been shown for many coronaviruses (31, 42, 54), including IBV (13), that replacement of the S ectodomain by that of another coronavirus results in viruses with the *in vitro* cell preference of the donor spike. Many, though not all, S glycoproteins are cleaved during synthesis into two subunits, the N-terminal S1 and the C-terminal S2 subunit (17, 36, 71). While S1 attaches the virion to the cell membrane by interacting with cell receptors, S2 is responsible for membrane fusion (12). For IBV, the receptor-binding domain has not yet been mapped, but as in other coronaviruses (29, 43, 65, 70), the cell binding determinants likely reside in the S1 subunit. Furthermore, the S1 domain is the main inducer of neutralizing antibodies and protective immune responses, and it displays a high level of variation (5 to 50%) between IBV strains (15, 16, 35, 37, 38, 59).

In general, the requirement for specific virus receptors on host cells restricts the coronaviral host repertoire. For many coronaviruses, but not for IBV, specific protein receptors have been elucidated. For IBV, attachment to and infection of host

* Corresponding author. Mailing address: Pathology Division, Department of Pathobiology, Faculty of Veterinary Medicine, Utrecht University, Yalelaan 1, 3584 CL Utrecht, The Netherlands. Phone: 31 30 253 4296. Fax: 31 30 253 2333. E-mail: m.h.verheije@uu.nl.

cells, both cultured cells (69) and *ex vivo* tracheal organ cultures (TOCs) (68), has been shown to depend on α2,3-linked sialic acid (α2,3-sia) (55). Only for IBV Beaudette, a strain with an extended host range in cell culture after serial passage in eggs (46, 50), has an additional host attachment factor, heparan sulfate, been resolved (46). However, since this strain has lost its ability to replicate in chickens (28, 33), the relevance of this host factor *in vivo* can be questioned. Because α2,3-sia is abundantly present in many different animal species, other, yet unknown determinants likely restrict the IBV host tropism. IBV may require a yet unidentified second receptor or another host factor in addition to α2,3-sia in order to enter cells. Alternatively, IBV may bind only to a very specific subset of α2,3-sialylated glycans, present only in chickens. Either way, IBV strain-dependent differences in tissue tropism might be explained by different preferences of the S proteins for α2,3-sia-containing glycans.

Since the binding of the IBV spike protein to host cells likely plays an important role in determining host and tissue tropism and thus the outcome of the infection, it is of particular interest to elucidate the characteristics of this interaction. To study these interactions, we decided to generate recombinant spike proteins, because most IBV strains are very limited in their ability to grow in cell culture and acquire genomic mutations rapidly as a result of cell culture adaptation (24). A similar recombinant protein approach has recently been taken to determine the receptor binding properties of hemagglutinin (HA) proteins of IAVs (23). Since both IBV and avian IAV are known to bind to α2,3-sialylated glycans, we first compared the interactions of recombinant S1 and HA proteins with avian tissues and glycans. In agreement with their different tropisms, the attachment proteins of IBV and IAV differed dramatically in avidity and specificity. Next, we analyzed the receptor binding of S proteins derived from IBV strains with reported differences in pathogenicity. Using histochemistry and glycan array analyses, we showed that the binding of these viral proteins correlates with their tissue tropisms and reflects the pathogenicities of these viruses *in vivo*.

MATERIALS AND METHODS

Genes and expression vectors. Gene sequences for IBV strains M41 (GenBank accession number AY851295), Beaudette CK (accession number AJ311317), H120 (accession number FJ888351), and B1648 (accession number X87238) were obtained from the National Center for Biotechnology Information (NCBI) GenBank (http://www.ncbi.nlm.nih.gov/genbank/). Human codon-optimized sequences of the S1-encoding domains (initiating directly downstream of the signal sequence and terminating at the furin cleavage site [amino acids {aa} 19 to 532 for IBV M41, IBV Beaudette, and IBV H120; aa 19 to 536 for IBV B1648]) were synthesized (GenScript) and cloned into the pCD5 vector (73). The S1 genes were preceded by a sequence encoding an N-terminal CD5 signal peptide and were followed by sequences encoding a C-terminal artificial GCN4 trimerization domain (RMKQIEDKIEEIESKQKKIENEIARIKKLVPRGSLE) (32) and *Strep*-tag II (WSHPQFEK; IBA GmbH) for affinity purification. An amino acid alignment of the IBV S1 domains was generated by neighbor-joining phylogeny (see Fig. 5A). The cloning of H5 (NCBI accession number ABW90137.1) from avian influenza virus H5N1 into pCD5 has been described previously (20).

Protein expression and purification. The pCD5 expression vectors containing the S1 domain-encoding sequences were transfected into HEK293T cells as described previously (11, 22). Tissue culture supernatants were harvested 7 days posttransfection. The S1 proteins were purified using *Strep*-Tactin Sepharose beads according to the manufacturer's instructions (IBA GmbH). Similarly purified culture supernatants of HEK293T cells transfected with a pCD5 plasmid lacking the S1 coding sequence served as negative controls. Where indicated, S1 proteins bound to *Strep*-Tactin beads were treated with *Vibrio cholerae* neur-

aminidase (VCNA) (2 μU/ml; Roche) for 3 h at 37°C, followed by three washing steps prior to the elution of the protein from the beads. The concentrations of the proteins were determined using the NanoDrop 1000 spectrophotometer (Thermo Fisher Scientific Inc.) and were confirmed by Western blotting. H5 of avian influenza virus H5N1 was expressed and purified similarly (20).

Western blotting. The expression and purification of the IBV S1 and IAV H5N1 HA proteins were analyzed by sodium dodecyl sulfate-polyacrylamide gel electrophoresis (SDS-PAGE) followed by Western blotting using the horseradish peroxidase (HRPO)-conjugated *Strep*-Tactin antibody (IBA GmbH). Where indicated, the S1 proteins were treated with peptide:*N*-glycosidase F (PNGase F; New England Biolabs Inc.) prior to electrophoresis according to the manufacturer's procedures in order to remove N-linked oligosaccharides.

Solid-phase assay. The binding of IBV S1 and IAV H5N1 HA was assessed by a fetuin binding assay. For this purpose, 100 μg/ml fetuin per well was used to coat 96-well Nunc MaxiSorp plates (Nalge Nunc International). Recombinant S1 or HA was precomplexed with an HRPO-linked anti-*Strep*-tag antibody (molar ratio, 2:1) for 30 min at 0°C prior to overnight incubation of limiting dilutions on the fetuin-coated plates. Binding was subsequently detected using a tetramethylbenzidine (TMB) substrate (BioFX) in an enzyme-linked immunosorbent assay (ELISA) reader (EL-808; Bio-Tek) by reading the optical density (OD) at 450 nm.

Spike and HA histochemistry. Formalin-fixed, paraffin-embedded tissues from a 6-week-old male broiler chicken and from a male barnacle goose (*Branta leucopsis*) were sectioned at a thickness of 4 μm. Tissue sections were deparaffinized and rehydrated, and antigens were retrieved by boiling in 10 mM sodium citrate (pH 6.0) for 10 min. Endogenous peroxidase was inactivated by 1% hydrogen peroxide in methanol for 30 min at room temperature (RT), and after washing with phosphate-buffered saline (PBS)–0.1% Tween (TPBS), the slides were blocked with 10% normal goat serum for 30 min at RT. To detect the binding of S1 protein to avian tissues, proteins (S1 at 100 μg/ml and H5 at 2 μg/ml) were precomplexed with *Strep*-Tactin-HRPO (1:200, IBA GmbH) for 30 min on ice before being applied to slides. After overnight incubation at 4°C, the slides were rinsed three times in PBS, and binding was visualized with 3-amino-9-ethyl-carbazole (AEC; Sigma-Aldrich). The tissues were counterstained with hematoxylin and were mounted with AquaMount (Merck). To check for nonspecific staining, slides were incubated with comparable volumes of similarly purified culture supernatants of HEK293T cells transfected with a pCD5 plasmid lacking the viral protein-encoding sequences. Images were captured using a charge-coupled device (CCD) camera and an Olympus BX41 microscope linked to Cell^B imaging software (Soft Imaging Solutions GmbH, Münster, Germany).

Where indicated, sialic acids were removed from the tissues by incubation of the slides with 1 mU VCNA for 20 h at 37°C before spike histochemistry was performed.

The ability of *Maackia amurensis* lectins (MAA lectins) to block the binding of S1 to tissues was studied by preincubating the slides with a range of concentrations (8 to 256 μg/ml) of nonconjugated MAAI and MAAII (Vector Laboratories Inc.) overnight at 4°C prior to performing spike histochemistry.

Lectin histochemistry. MAA lectins were used to detect α2,3-linked sialic acids. Biotin-labeled MAAI and MAAII (Vector Laboratories Inc.) were applied to formalin-fixed, paraffin-embedded tissues after antigen retrieval and endogenous peroxidase blocking as described under "Spike and HA histochemistry" above. After blocking with 10% normal goat serum for 30 min at RT, lectins were applied to the slides at 7 μg/ml and were incubated overnight at 4°C. Next, the slides were washed three times in TPBS and were subsequently incubated with peroxidase-conjugated avidin for 30 min using the Vector ABC kit (Vector Laboratories Inc.). Peroxidase was revealed with AEC (Sigma-Aldrich), and after counterstaining with hematoxylin, the tissues were mounted with Aqua-Mount (Merck). Images were captured using a CCD camera and an Olympus BX41 microscope linked to Cell^B imaging software (Soft Imaging Solutions GmbH).

Glycan array analysis. Microarray printing has been described previously (9). Printed slides of the Consortium for Functional Glycomics (CFG) glycan library (CDC versions 4.1 and 4.2) (see Table S1 in the supplemental material for the glycans represented) were used in these experiments. Ligand profiling of IBV S1 proteins and IAV H5N1 HA was performed essentially as reported elsewhere (62). Briefly, recombinant proteins (200 μg/ml) were precomplexed with an HRPO-linked anti-*Strep*-tag antibody (molar ratio, 2:1) for 30 min at 0°C prior to incubation for 60 min on the microarray slide under a microscope cover glass in a humidified chamber at RT. Microarray slides were subsequently washed by successive rinses in TPBS and were overlaid with an Alexa Fluor 488-coupled secondary antibody. After repeated washes with TPBS, PBS, and deionized water, the slides were immediately subjected to imaging (9).

RESULTS

Expression, purification, and biological activity of IBV M41 S1 and IAV H5N1 HA proteins. Receptor binding properties can be successfully studied using a recombinant protein approach, as has recently been demonstrated for the hemagglutinin (HA) of influenza A virus strains (23). To investigate the interactions between IBV and the host, we took a similar approach by cloning the codon-optimized sequence of the S1 gene of the virulent Massachusetts reference strain M41 (14) into a pCD5 expression vector, where it was preceded by the CD5 signal peptide and followed by sequences encoding the GCN4 trimerization domain and *Strep*-tag II (Fig. 1A). The proteins were expressed by transfection of human HEK293T cells, and proteins secreted into the medium were purified using *Strep*-tag technology (IBA GmbH, Münster, Germany). In parallel, we expressed and purified the HA glycoprotein of the highly pathogenic avian influenza virus H5N1 subtype in a manner similar to that described previously (20). The resulting proteins were analyzed by Western blotting using the *Strep*-Tactin antibody either before or after PNGase F treatment. M41 S1 migrated around 105 kDa on an SDS-PAGE gel (Fig. 1B), and removal of the N-linked glycans with PNGase F increased the electrophoretic mobility of S1 to around 70 kDa. Thus, the S1 proteins are highly glycosylated, as expected (71). The recombinant HA protein was also glycosylated; it migrated at around 60 kDa after removal of its N-linked glycans. The oligomeric states of HA and S1 were confirmed by blue native PAGE analysis and gel filtration column chromatography (data not shown) (20). In conclusion, soluble oligomeric glycosylated IBV S1 proteins can be expressed and purified as previously described for HA.

To compare the biological activity of M41 S1 with that of HA, we determined the ability of S1 to bind to sialylated glycans present on bovine fetuin, a blood glycoprotein that contains both N-linked and O-linked sialylated glycan side chains. Fetuin has been shown to provide a good substrate for analysis of the receptor binding properties, and hence the tropism determinants, of various influenza virus HA proteins (23). Recombinant HA and S1 were precomplexed with an anti-*Strep*-tag antibody, as described in Materials and Methods, before a solid-phase binding assay was performed. To our surprise, no binding of M41 S1 was detected, in contrast to HA, which displayed concentration-dependent binding to fetuin (Fig. 1C). It is likely that either sialylated glycan side chains present on the fetuin are not recognized by the spike of IBV or the avidity of S1 for fetuin is below the detection level. Comparable results were obtained when we investigated binding to glycophorin, another blood protein containing mainly O-linked sialylated glycans (data not shown).

Next, we decided to investigate the binding characteristics of these proteins with more natural substrates. To this end, we used tissues of the chicken respiratory tract, the primary target organ of both IBV and avian influenza virus. Slides were prepared from formalin-fixed, paraffin embedded trachea and lung tissues from a 6-week-old broiler chicken. In histochemistry, we applied the soluble recombinant S1 and HA proteins after precomplexing them with HRPO-linked *Strep*-Tactin. For M41 S1, binding to both the chicken trachea and lung could readily be observed. In particular, M41 S1 bound to the base of
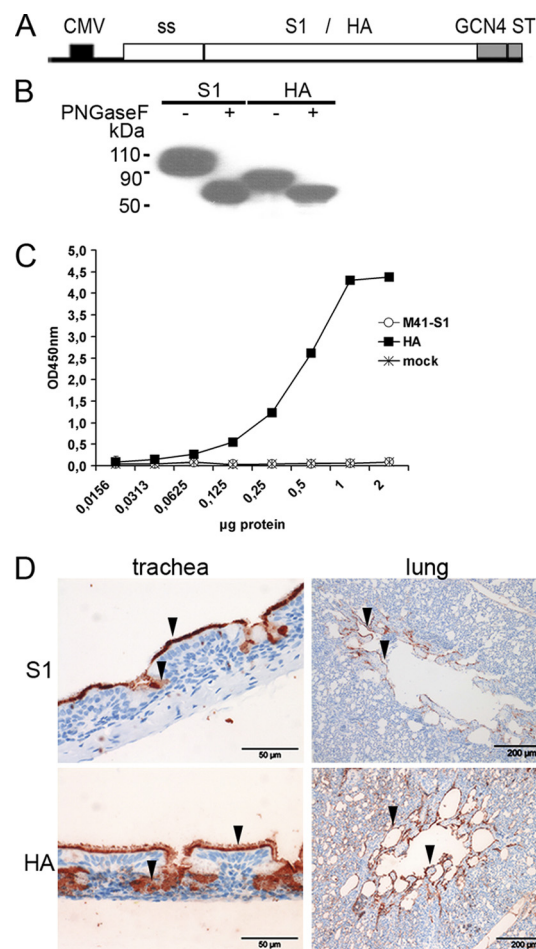

FIG. 1. Expression of recombinant IBV S1 and H5N1 HA proteins. (A) Schematic representation of the S1 and HA expression cassettes. The S1 or HA ectodomain-encoding sequences were cloned in frame with DNA sequences coding for a signal sequence (ss), the GCN4 isoleucine zipper trimerization motif, and *Strep*-tag II (ST) under the control of a cytomegalovirus (CMV) promoter. (B) S1 proteins expressed in HEK293T cells and purified from the culture medium were analyzed by SDS-PAGE followed by Western blotting using *Strep*-Tactin. Where indicated, the samples were treated with PNGase F prior to electrophoresis. (C) Fetuin binding was analyzed by a solid-phase binding assay as described in Materials and Methods. The graph shows the results of an independent experiment performed in triplicate. (D) Spike and HA histochemistry was performed by incubating chicken trachea and lung tissues with *Strep*-Tactin-precomplexed M41 S1 (5 μg) or H5N1 HA (0.1 μg) as described in Materials and Methods. Binding is indicated by arrowheads.

the cilia of the epithelial cells lining the surface of the trachea, as well as to the mucus-producing goblet cells (Fig. 1D). In the chicken lung, M41 S1 attached specifically to parabronchial epithelial cells (Fig. 1D). The cells to which S1 bound were previously reported to be sensitive to IBV (1, 68) and corresponded to the pathological lesions observed after IBV infection *in vivo* (1, 6, 7), indicating that the binding of S1 was specific. No staining was observed when the tissue slides were incubated with similarly purified culture supernatants of cells transfected with an empty vector (data not shown). The binding specificity of HA for the chicken trachea and lung closely resembled that of M41 S1 (Fig. 1D), while additional binding

of HA to the tips of the cilia of the tracheal epithelium was observed. Interestingly, the amount of HA protein required for binding in histochemistry was considerably less than the amount of M41 S1 required (0.1 and 5 μg per section, respectively), in agreement with previously reported data on the binding of influenza virus and IBV to TOCs (69). When HA proteins expressed in a cell line lacking the ability to generate sialylated N-glycans (thereby more closely resembling the glycosylation state of virion-associated HA in the presence of neuraminidase) were applied, the avidity of HA for tissues increased further (data not shown) (22). In conclusion, recombinant soluble protein histochemistry provides an attractive means to study the binding characteristics of viral attachment proteins. Furthermore, our data show that the IBV S1 protein is functional and that the lack of detectable binding of M41 S1 in the fetuin solid-phase assay (Fig. 1C) might be due to low avidity for this substrate.

Viral protein specificity for sialic acids of the chicken respiratory tract. For both IBV and avian IAV, it is known that α2,3-sialylated glycans on host cells play a role in virus infection. To investigate the contribution of α2,3-sia to the attachment of M41 S1 and IAV HA to the chicken respiratory tract, we pretreated the tissue slides with *Vibrio cholerae* neuraminidase (VCNA) to cleave off tissue-bound α2,3-sia before performing histochemistry. The binding of M41 S1 to chicken trachea and lung tissues was completely abolished after VCNA treatment (Fig. 2A), indicating that M41 S1 requires sialic acids as host factors for attachment to the chicken respiratory tract. For HA, a marked reduction of staining of the trachea and the air capillaries of the lung (Fig. 2A) was observed. HA binding could not, however, be completely prevented, likely due to incomplete removal of sia in combination with the high avidity of HA for the chicken respiratory tract.

We next compared the attachment patterns of the viral proteins with those of *Maackia amurensis* lectins (MAA lectins) detecting α2,3-sia. Because differences in tissue distribution have been observed for different isoforms of MAA lectins (49), we used both biotinylated MAAI and MAAII in our study. For MAAI, binding to the cilia of the epithelial cell layer, as well as weak binding to the mucus-producing goblet cells of the trachea, was observed, while MAAII had a more profound avidity for tracheal goblet cells (Fig. 2B). Clear differences in the binding of MAAI and MAAII to the lower respiratory tract were observed. While MAAI preferentially bound to the parabronchial epithelium, MAAII rather bound to connective tissue within the chicken lung (Fig. 2B). Therefore, the binding of MAAI to the chicken respiratory tract more closely resembled that of M41 S1 and IAV HA.

Finally, we investigated the ability of MAAI to block the binding of M41 S1 to the chicken respiratory tract by preincubating tissue slides with nonbiotinylated MAAI. M41 S1 binding to the trachea and lung could be completely blocked using 64 μg/ml of MAAI (Table 1). Interestingly, lower concentrations of MAAI blocked M41 S1 attachment only to the goblet cells, not to the epithelial cells of the trachea. In the lung, 8 μg/ml MAAI was already sufficient to completely block M41 S1 binding. Taken together, these data show that IBV M41 S1, just like avian IAV HA (22), binds to chicken tissue in an α2,3-sia dependent manner and functions as a lectin.
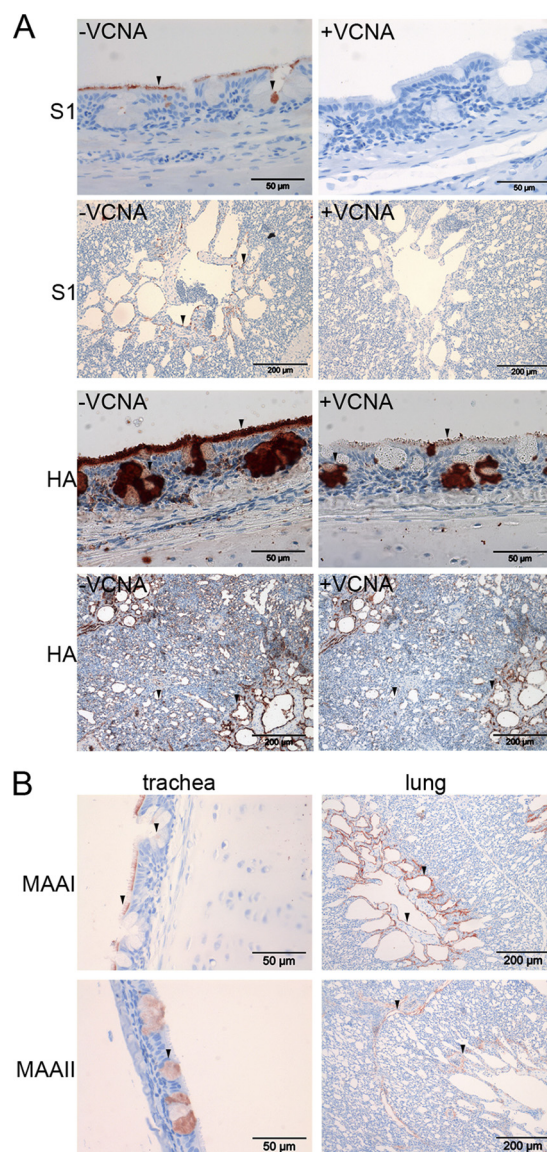

FIG. 2. Histochemistry of the spike protein and lectins on chicken respiratory tract tissues. (A) Chicken respiratory tract tissue slides were pretreated with PBS alone (−VCNA) or PBS with VCNA (+VCNA) before spike and HA histochemistry was performed. (B) Lectin histochemistry was performed by incubating chicken trachea or lung tissue slides with biotinylated lectin MAAI or MAAII. Binding is indicated by arrowheads.

Host-specific binding of IBV M41 S1 and H5N1 IAV HA. IBV and IAV both prefer binding to α2,3-linked sialic acids; however, their host tropisms differ markedly. While IBV infection is restricted to domestic fowl, IAV infections can occur in many different species. To investigate whether the reported differences in the host tropisms of these viruses might be explained by species-specific binding to the respiratory tract, we compared the attachment of M41 S1 and IAV HA to the respiratory tract of a barnacle goose. By histochemistry, we observed that M41 S1 was able to bind to goblet cells and mucus covering the epithelium of the goose trachea; however, no specific binding to the cilia of the epithelial cells was ob-

TABLE 1. Blocking of M41 S1 binding to chicken respiratory tract tissues[a]

Tissue type	Tissue(s) to which M41 S1 (5 μg/ml) bound in the presence of MAAI at the following concn (μg/ml)[b]:				
	0	8	16	32	64
Trachea	Goblet cells/cilia	Cilia	Cilia	Cilia	—
Lung	Epithelium	—	—	—	—

[a] Tissue slides were preincubated with various concentrations of nonbiotinylated MAAI lectin before the application of *Strep*-Tactin-precomplexed M41 S1. No binding was observed in the presence of 64 μg/ml MAAI.
[b] —, no binding.

served (Fig. 3). In the lung, no binding of M41 S1 to the goose parabronchial epithelium was detected (Fig. 3), in contrast to what was observed for the chicken lung (Fig. 1D), although some staining of the goose primary bronchus could be observed (not shown). In contrast, HA was able to bind with high avidity to both the cilia and the goblet cells of the goose trachea and to the epithelium of primary and secondary bronchi and parabronchi. Taken together, our data suggest that the inability of IBV M41 to infect a goose can (at least partly) be explained by the restricted binding of the spike proteins to the goose respiratory epithelial cells.

Fine glycan specificity of M41 S1 and H5N1 HA. To elucidate the fine receptor specificity of M41 S1, we next characterized its oligosaccharide binding specificity by performing glycan array analysis (in collaboration with the Consortium for Functional Glycomics [http://www.functionalglycomics.org/static/index.shtml]). To this end, soluble M41 S1 was precomplexed with the *Strep*-tag II antibody, and binding to printed slides representing more than 450 glycans (see Table S1 in the supplemental material) was detected using a fluorescein isothiocyanate (FITC)-conjugated secondary antibody. The binding profile revealed that M41 S1 specifically recognized only one sialic acid-containing glycan: Neu5Acα2,3Galβ1,3(Neu5Acα2,3Galβ1,4)-GlcNAc (Fig. 4; see also Table S1, column M41 S1). Although this α2,3-disialoside was the only substrate recognized, we cannot exclude the possibility that M41 S1 binding to respiratory tissues also involves other
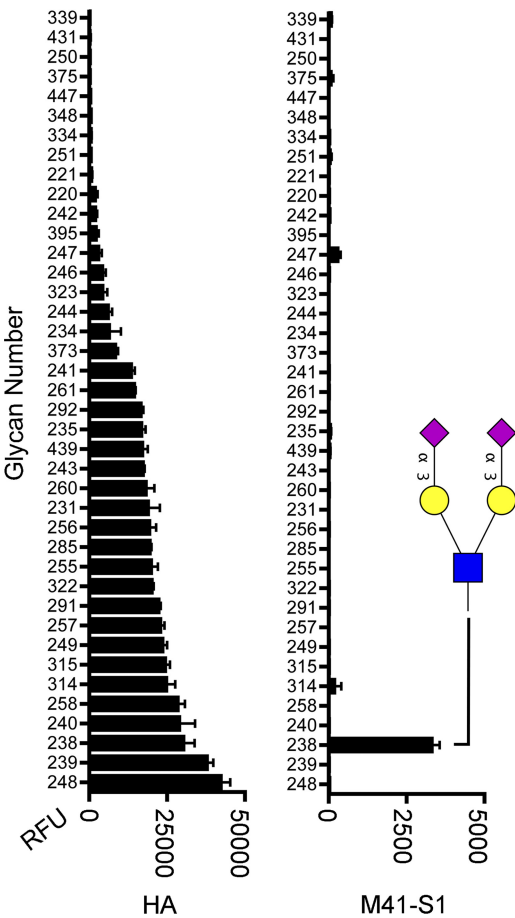

FIG. 4. Glycan array analysis of M41 S1 and H5N1 HA. Recombinant M41 S1 and H5N1 HA proteins were precomplexed with *Strep*-tag antibodies and were then incubated on glycan array slides. Glycan numbers are given on the *y* axis; glycans are sorted according to the binding profile of H5N1 HA. The structure of the glycan recognized by M41 S1 (generated with GlycoWorkbench [10]) is depicted. The complete glycan array results, as well as the identities of all glycans, are shown in Table S1 in the supplemental material. RFU, relative fluorescence units.
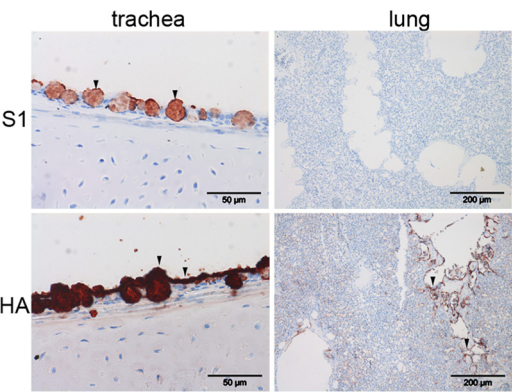

FIG. 3. Histochemistry of M41 S1 and H5N1 HA on goose respiratory tissues. Spike and HA histochemistry was performed by incubating barnacle goose trachea and lung tissues with *Strep*-Tactin-precomplexed M41 S1 (5 μg) or H5N1 HA (0.1 μg) as described in Materials and Methods. Binding is indicated by arrowheads.

sialic acid-containing moieties that are not represented on the glycan array.

Next, we compared the fine receptor specificity of M41 S1 with that of IAV HA expressed in HEK293 GnTI cells, which are impaired in glycosylation, to mimic the *in vivo* situation most closely. The HA protein demonstrated binding to many different glycans (Fig. 4; see also Table S1 in the supplemental material, column H5N1 HA), consisting of type 1 and type 2 chain glycans containing α2,3-linked sialic acids (as expected [27, 64]). Furthermore, the avidity of HA binding to glycans was much higher than that of M41 S1 binding (Fig. 4, compare relative fluorescence units [RFU] for IAV H5N1 HA versus M41 S1), in agreement with the observed differences in histochemistry. In conclusion, while M41 S1 has relatively low avidity for sialic acid-containing glycans, it has markedly high fine receptor specificity.

Binding of IBV S1 proteins to chicken tissues reflects virus growth *in vivo*. Our spike histochemistry assay is a feasible assay with which to investigate the binding characteristics of
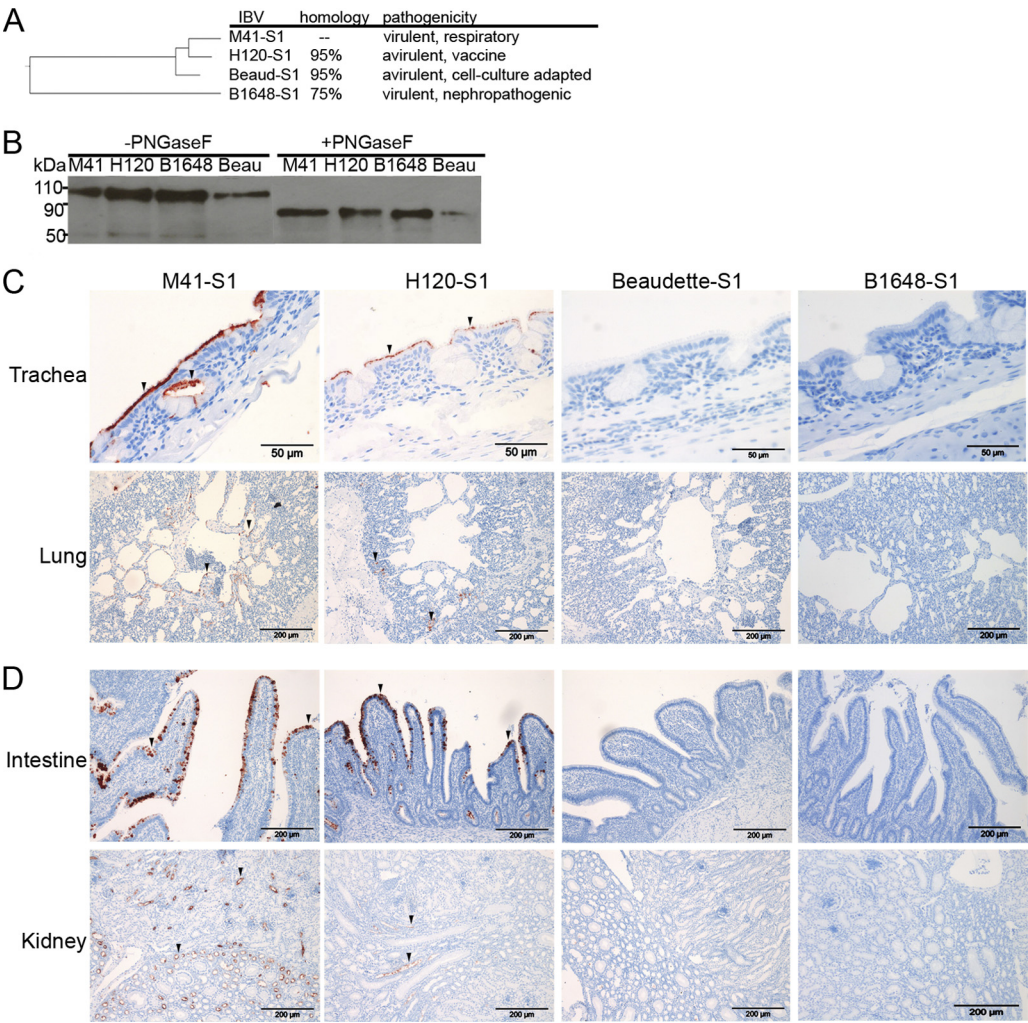
FIG. 5. Expression of recombinant IBV S1 proteins and spike histochemistry. (A) Summary of the S1 amino acid sequences of M41, H120, Beaudette, and B1648. The percentages of amino acid similarity with the reference strain M41 and the reported pathogenicity profiles are shown. (B) S1 proteins expressed in HEK293T cells and purified from the culture medium were analyzed by SDS-PAGE, followed by Western blotting using *Strep*-Tactin. Where indicated, the samples were treated with PNGase F prior to electrophoresis. (C and D) Spike histochemistry was performed by applying similar amounts of precomplexed M41 S1, H120 S1, Beaudette S1, and B1648 S1 to sections of chicken trachea or lung tissue (C) or intestine or kidney tissue (D). Binding is indicated by arrowheads.

the IBV spike protein. Therefore, we decided to expand our investigation by comparing the binding features of S1 proteins of IBV strains with differences in pathogenicity. We chose four IBV strains with reported differences in clinical symptoms in chickens as representative examples: in addition to the virulent Massachusetts strain M41 (14), we focused on the S1 proteins of the Massachusetts vaccine strain H120 (8), the avirulent and cell culture-adapted Massachusetts strain Beaudette (5), and the nephropathogenic strain B1648 (48, 51). Although the pathogenicity profiles of these strains differ markedly *in vivo*, their S1 proteins share 75 to 95% sequence identity (summarized in Fig. 5A).

To allow the expression of their S1 proteins as soluble proteins, codon-optimized sequences of all S1 genes were cloned into the pCD5 expression vector, and proteins were produced and purified in a manner similar to that described for M41 S1. The resulting proteins were analyzed by Western blotting using

the *Strep*-Tactin antibody either before or after PNGase F treatment. All S1 proteins displayed similar electrophoretic mobilities, migrating at around 105 kDa in SDS-PAGE (Fig. 5B), and they appeared to be glycosylated to a similar extent as M41 S1 (Fig. 5B, +PNGaseF).

We then compared the binding characteristics of M41 S1 with those of the related but avirulent S1 proteins of the Massachusetts strains H120 and Beaudette for the chicken respiratory tract. Both H120 and Beaudette are generated by serial passage (120 and at least 250 passages, respectively) in embryonated eggs and are considered nonpathogenic for chickens. However, while H120 is a widely used vaccine strain (8), Beaudette has almost completely lost its capacity to replicate *in vivo* (28). Spike histochemistry was performed by applying similar amounts of S1 proteins (5 μg per section). We observed that H120 S1 bound to the trachea and the lung with much lower avidity than M41 S1 (Fig. 5C). In particular, weak

staining of the cilia, but no binding to goblet cells, was observed in the trachea. In the lung, only minor staining of epithelial cells in the air capillaries could be detected. For Beaudette S1, no binding to the respiratory tract could be detected at all (Fig. 5C), even when a 5-fold-larger amount of protein was used (data not shown). In conclusion, the binding avidities of the Massachusetts S1 proteins investigated correlate with the reported differences in virus growth of the respective IBVs *in vivo*. Furthermore, our data suggest that even a few mutations in the S1 gene, which have likely arisen by serial passage of IBV in eggs, can alter the binding avidity of S1 proteins for chicken tissues. This was in line with our glycan array data, showing that both H120 S1 and Beaudette S1 lost their abilities to bind to Neu5Acα2,3Galβ1,3(Neu5Acα2,3Galβ1,4)-GlcNAc, without gaining specificity for other glycans (see Table S1 in the supplemental material, columns H120 S1 and Beaudette S1). Whether the binding of H120 to tissues, but not to the glycan array, is due to differences in the sensitivities of these assays or to the restricted representation of glycans on the array remains to be elucidated.

Since IBV has been isolated from the intestine (53), and sialic acids are abundantly present in the gut (30), we next investigated the binding of S1 proteins to intestinal tissue. For both M41 S1 and H120 S1, binding mainly to mucus-producing goblet cells was observed (Fig. 5D). Noticeably higher avidity of H120 S1 for those cells was observed, as demonstrated by the higher intensity of staining when similar amounts of S1 proteins were used. Likely, since IBV replication in the chicken gut usually does not result in clinically evident disease (15), the binding of H120 S1 to sialic acid-rich intestinal mucins might facilitate virus excretion via the feces. As with the respiratory tract, no binding of Beaudette S1 could be observed.

Strikingly, in none of the tissues investigated could any appreciable binding of the more diverse B1648 S1 protein be detected (Fig. 5C). Because IBV B1648, after respiratory infection, induces severe nephropathogenicity (51), we next decided to compare its binding to kidney tissue with that of M41. M41 replication in the kidney has been reported; however, this usually does not result in renal disease (7). In accordance with the fact that the cells support M41 replication *in vivo* (7), M41 S1 showed clear binding to epithelial cells of the distal convoluted tubules in the cortex and to thick segments of the medullary loops by histochemistry (Fig. 5D). Again, and unexpectedly, no attachment of B1648 S1 to the kidney could be detected (Fig. 5D).

Role of sialic acids in the attachment of the spike protein to tissues. While the Massachusetts S1 proteins have highly similar amino acid sequences, the S1 domain of B1648 is more divergent from M41 S1 than the others, with 75% rather than 95% amino acid identity. One other remarkable observation made for several nephropathogenic strains is their poor hemagglutination ability (S. de Wit, personal communication); while M41 can hemagglutinate red blood cells, the ability of nephropathogenic strains to do so seems to be severely hampered. Since the ability to hemagglutinate is affected by the presence of sialic acids on the virion, usually requiring pretreatment with neuraminidase, we decided to investigate the contribution of sialic acids on S1 proteins to their binding to tissues. To this end, M41 and B1648 S1 proteins were treated with VCNA to remove sialic acids before spike histochemistry
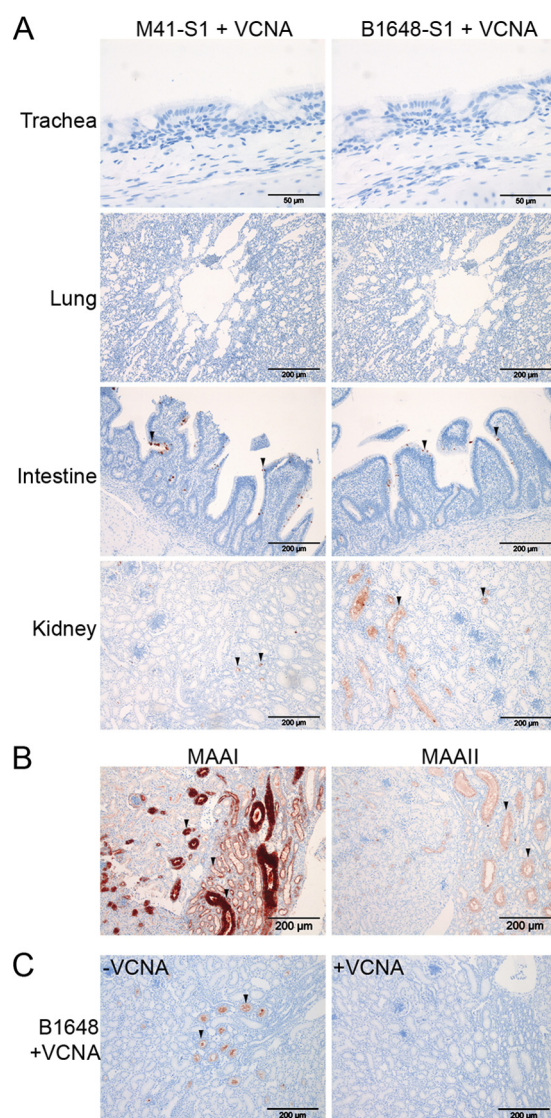

FIG. 6. Spike histochemistry of neuraminidase-treated M41 S1 and B1648 S1 on chicken tissues. (A) S1 proteins of M41 and B1648 were pretreated with *Vibrio cholerae* neuraminidase before they were applied to chicken trachea, lung, intestine, and kidney slides. (B) Lectin histochemistry using biotinylated MAA lectins on kidney tissues. (C) Kidney tissue was pretreated with VCNA to remove α2,3-linked sia before VCNA-treated B1648 S1 was applied. Binding is indicated by arrowheads.

was performed. For M41 S1, treatment with VCNA resulted in complete loss of binding to epithelial and goblet cells of the respiratory tract, while only some residual staining, indicating binding to goblet cells of the intestine and to some medullary loops in the kidney, was observed (Fig. 6A). In contrast, after VCNA treatment, B1648 S1 acquired binding both to intestinal mucus-producing cells and to kidney tissue. In particular, this protein bound specifically to cells of the mucus-secreting collecting tubules and collecting ducts in the medulla (Fig. 6A); these cells did not bind M41 S1. Thus, while the sialic acids present on the M41 spike protein are required for binding, they actually appear to block the binding of B1648 S1 to tissues. Strikingly, VCNA-treated B1648 S1 did not bind to the

chicken respiratory tract (Fig. 6A), perhaps due to low avidity for host factors present on those cells. In a parallel experiment, we determined whether the presence of sialic acids on Beaudette S1 also blocked its ability to bind to tissue slides. After VCNA treatment of this S1 protein, however, no gain of binding to any of the tissues was observed (data not shown).

To further elucidate the nature of the binding ligands of B1648 S1, we first compared the binding of VCNA-treated B1648 with MAA lectin staining of the chicken kidney. MAAI displayed strong binding to convoluted tubes and collecting tubules, but binding to glomeruli and medullary loops was also observed (Fig. 6B). MAAII binding was more specific for convoluted tubules in the cortex and collecting ducts and tubules, thus resembling the binding of B1648 S1 to the kidney more closely than MAAI binding. Subsequent blocking of kidney slides with unlabeled MAAII before application of the VCNA-treated B1648 protein showed that 264 μg/ml MAAII was required to completely block the binding of B1648 S1 (data not shown), indicating again that this spike protein could serve as a lectin. To confirm the involvement of α2,3-sia in B1648 S1 binding, kidney slides were pretreated with VCNA before the application of VCNA-pretreated B1648 S1. The lack of binding after treatment (Fig. 6C) clearly demonstrated that attachment was α2,3-sia dependent. Finally, the specific glycan binding profile of VCNA-treated B1648 S1 was investigated by glycan array. Unfortunately, no specific binding to any of the glycans present on the array could be detected (see Table S1 in the supplemental material, column B1648 S1 + VCNA). Notwithstanding, our data provide evidence to explain the reported differences in the tissue tropisms and pathogenicities of those viruses for the host.

DISCUSSION

In this study we have used a comparative approach to investigate the binding characteristics of the S1 protein of avian coronavirus IBV strains with reported differences in both organ tropism and pathogenicity. Spike histochemistry demonstrated that the attachment patterns of S1 proteins resembled the reported cell and tissue tropisms of the corresponding strains. Moreover, the binding affinities of IBV Massachusetts strains correlated with their reported pathogenicity profiles *in vivo*. Finally, the observed differences in the binding of IBV S1 and the HA protein of influenza virus H5N1 to various avian tissues and glycans resemble the distinct preferences of these viruses for avian hosts.

Sialic acids are important for establishing an IBV infection in cells *in vitro* (1, 68, 69); however, the exact requirements for this interaction had not been elucidated until now. Here we have demonstrated that the IBV spike protein interacts, in a sialic acid-dependent way, with tissues of a susceptible host. In particular, all binding S1 proteins used α2,3-sialylated substrates, as evidenced by the fact that attachment could be inhibited by pretreating the slides with VCNA or by preincubating them with MAA lectins, which preferentially bind to α2,3-sialidated oligosaccharides. α2,3-Sialic acids are present in the chicken trachea (26, 52), the lower respiratory tract (1), the intestine (52), and the kidney (this study); however, interpretation of lectin histochemistry data is difficult due to differences in the binding of MAA isoforms and lectins from differ-

ent suppliers (49; our data). Thus, although lectin histochemistry is widely used to gain insight into virus-host interactions, it appears limited in determining fine glycan specificity. With the recently developed glycan microarray technology, receptor specificities can be studied in more detail (9, 63); this technology allowed us to identify one particular α2,3-disialylated glycan as a fine receptor ligand of M41 S1. It will be of interest to test whether this glycan has the ability to block IBV infection. To our knowledge, no studies have yet analyzed specific N-linked glycan modifications in avian tissues, except for the chorioallantoic and amniotic cells of embryonated eggs (61), from which the disialoside identified in this study was not reported. To ultimately correlate the host and tissue tropisms of IBV with the tissue distribution of specific glycans, a better understanding of avian glycobiology is required.

Although IBV and avian influenza virus both prefer binding to α2,3-linked sialic acids, their host tropisms are markedly different. While IBV has a very narrow species tropism, infecting only chickens, avian influenza virus infects many different avian species. In contrast to IAV, IBV does not contain neuraminidase activity to regulate *in vivo* binding (58). Therefore, it must have evolved other mechanisms to avoid being trapped by mucins covering the epithelium. When the affinities of IBV S1 and HA derived from IAV H5N1 (which possesses neuraminidase activity to cleave off bound sialic acids *in vivo*) were compared, the relatively low avidity of S1 became evident (69; this study [10-fold-lower avidity in the glycan array and 50-fold-lower avidity by histochemistry]). Furthermore, glycan array analyses indicate that M41 S1 has a high specificity for glycans; it bound to only one distinct α2,3-disialylated N-glycan, while HA recognized many different α2,3-linked sialic acids (27, 64; this study). Therefore, we suggest that the low avidity and high specificity of IBV S1 for sialic acids might contribute to the restricted host tropism of IBV.

Our data suggest that sialic acid binding of the S1 domain of IBV may be a determinant for the *in vivo* growth and tropism of IBV. Although sialic acid binding appears to be a conserved feature of IBV (1, 68, 69; this study), differences in avidity and preferences for specific sialoconjugates explain, at least partly, the observed *in vivo* pathotypes. While the observed differences in binding are in agreement with the reported growth differences of IBV strains *in vivo*, strikingly, only minor differences between virus strains have been reported in TOCs (19, 33, 68). This discrepancy between S1 binding and TOC infection may be due to the differences in the sensitivities of these assays, since low-avidity binding to sialic acids might be sufficient to establish a TOC infection but below the detection limit of our assay. Otherwise, other viral proteins may contribute to TOC infection. In particular, a role for the S2 domain of Beaudette is proposed, since its extended tropism *in vitro* has been associated with a predicted heparin-binding site in this domain (46), and no binding of Beaudette S1 to cultured cells known to be sensitive to Beaudette could be observed (data not shown). We are currently developing a full-length spike expression system in order to investigate whether this domain contributes to binding to cells. Despite the differences in the assays, our data indicate that limited amino acid changes (M41, H120, and Beaudette are 95% identical) are sufficient to change the avidity of binding to tissues and glycans. For H5N1, a few amino acid mutations in the hemagglutinin appeared to

be sufficient to change the attachment pattern (18) and sialic acid preference (23, 66). Whether IBV strains with altered sialic acid preferences will evolve remains to be seen.

A role for the spike protein in determining IBV tissue and host tropism has been suggested previously, since egg-adapted viruses, which are attenuated in adult chickens, accumulate mutations predominantly in the spike protein (3, 24, 45). The role of the spike in determining tropism is further underscored in studies reporting that spike mutations due to selective pressure in various adult chicken tissues cause a phenotypic shift (25) or reversion to virulence of vaccine strains (34, 47, 67). However, since these viruses accumulated mutations not only in the spike but also in other parts of the viral genome, the exact role of the spike protein in determining tropism and pathogenicity remains to be elucidated. Other studies indeed suggest that the S1 domain is not the only viral determinant of the clinical outcome. It has been shown that the presence of the virulent M41 spike ectodomain was not sufficient to confer pathogenicity on a recombinant Beaudette virus *in vivo* (33) but that the IBV replicase proteins contribute to the pathogenicity of IBV in chickens (4).

Interestingly, while removal of sialic acids from the S protein derived from nephropathogenic IBV was required for tissue binding, the same treatment of the M41 and H120 S proteins abolished binding; for Beaudette, the presence of sialic acids on the spike appeared not to be the reason for the lack of binding. This discrepancy is puzzling, and rather unexpected, since the glycosylation of all S1 expressed proteins seemed to be comparable (Fig. 5B). Although the possibility cannot be formally excluded, we do not consider it very likely that our results would be much affected by the expression system used, since avian and mammalian cells synthesize glycoproteins carrying very similar oligosaccharides (2). Perhaps there are yet unresolved differences in glycosylation and/or sialylation of the S1 proteins of various IBV strains that are involved in providing a proper conformation for binding to cells (39). While all S1 proteins investigated contain 18 potential N-glycosylation sites, two of these sites are located farther upstream in B1648 S1 than in the other S1 proteins. If these sites are occupied, the glycan might block the receptor binding site of B1648 when sialylated. It might well be, also, that the respective sialic acid binding sites of the various IBV S1 proteins differ, with concomitant changes in binding characteristics. Since the receptor binding domain for IBV has not been identified yet, this possibility awaits further investigation.

For several other coronaviruses, a contribution of sialic acid binding to pathogenicity has been reported previously. The enteropathogenicity of transmissible gastroenteritis virus (TGEV) in piglets (40, 41) has been associated with the presence of sialic acid binding sites in the spike (56), whereas the serologically related porcine respiratory coronavirus (PRCV), devoid of such binding sites, lacked the ability to cause enteric disease. In striking contrast to IBV and TGEV, other coronaviruses that bind sialic acids, for example, bovine coronavirus (BCoV) and some mouse hepatitis coronavirus (MHV) strains, do contain acetylesterase (HE) activity to regulate their sialic acid binding *in vivo* (reviewed in reference 57). For these viruses, temperature-dependent HE activity (BCoV [44]) and levels of HE expression (MHV [72]) seemed to correlate with preferred virus replication sites *in vivo* and pathogenicity.

In conclusion, our study revealed intriguing differences between the spike characteristics of IBV strains with different pathogenicities and showed that IBV S1 attachment patterns can be used to predict and explain viral tropism. Our S1 proteins are excellent tools for the further dissection of spike-host interactions and for the elucidation of parallels and differences between IBV strains, but also between other avian viruses, as demonstrated here by the HA protein binding of avian influenza virus H5N1.

REFERENCES

1. **Abd El Rahman, S., C. Winter, A. El-Kenawy, U. Neumann, and G. Herrler.** 2010. Differential sensitivity of well-differentiated avian respiratory epithelial cells to infection by different strains of infectious bronchitis virus. J. Virol. **84:**8949–8952. doi:10.1128/JVI.00463-10.
2. **Aich, U., et al.** 2011. Glycomics-based analysis of chicken red blood cells provides insight into the selectivity of the viral agglutination assay. FEBS J. **278:**1699–1712. doi:10.1111/j.1742-4658.2011.08096.x.
3. **Ammayappan, A., C. G. J. Upadhyay, Jr., and V. N. Vakharia.** 2009. Identification of sequence changes responsible for the attenuation of avian infectious bronchitis virus strain Arkansas DPI. Arch. Virol. **154:**495–499.
4. **Armesto, M., D. Cavanagh, and P. Britton.** 2009. The replicase gene of avian coronavirus infectious bronchitis virus is a determinant of pathogenicity. PLoS One **4:**e7384.
5. **Beaudette, F. R., and C. B. Hudson.** 1937. Cultivation of the virus of infectious bronchitis. J. Am. Vet. Med. Assoc. **90:**51–60.
6. **Benyeda, Z., et al.** 2009. Comparison of the pathogenicity of QX-like, M41 and 793/B infectious bronchitis strains from different pathological conditions. Avian Pathol. **38:**449–456. doi:10.1080/03079450903349196.
7. **Benyeda, Z., et al.** 2010. Comparative histopathology and immunohistochemistry of QX-like, Massachusetts and 793/B serotypes of infectious bronchitis virus infection in chickens. J. Comp. Pathol. **143:**276–283. doi:10.1016/j.jcpa.2010.04.007.
8. **Bijlenga, G., J. K. Cook, J. Gelb, Jr., and J. J. de Wit.** 2004. Development and use of the H strain of avian infectious bronchitis virus from the Netherlands as a vaccine: a review. Avian Pathol. **33:**550–557. doi:10.1080/03079450400013154.
9. **Blixt, O., et al.** 2004. Printed covalent glycan array for ligand profiling of diverse glycan binding proteins. Proc. Natl. Acad. Sci. U. S. A. **101:**17033–17038. doi:10.1073/pnas.0407902101.
10. **Bohne-Lang, A., and C. W. von der Lieth.** 2005. GlyProt: in silico glycosylation of proteins. Nucleic Acids Res. **33:**W214–W219. doi:10.1093/nar/gki385.
11. **Bosch, B. J., et al.** 2010. Recombinant soluble, multimeric HA and NA exhibit distinctive types of protection against pandemic swine-origin 2009 A(H1N1) influenza virus infection in ferrets. J. Virol. **84:**10366–10374. doi:10.1128/JVI.01035-10.
12. **Bosch, B. J., R. van der Zee, C. A. de Haan, and P. J. Rottier.** 2003. The coronavirus spike protein is a class I virus fusion protein: structural and functional characterization of the fusion core complex. J. Virol. **77:**8801–8811.
13. **Casais, R., B. Dove, D. Cavanagh, and P. Britton.** 2003. Recombinant avian infectious bronchitis virus expressing a heterologous spike gene demonstrates that the spike protein is a determinant of cell tropism. J. Virol. **77:**9084–9089.
14. **Cavanagh, D.** 1981. Structural polypeptides of coronavirus IBV. J. Gen. Virol. **53:**93–103.
15. **Cavanagh, D.** 2007. Coronavirus avian infectious bronchitis virus. Vet. Res. **38:**281–297.
16. **Cavanagh, D., and P. J. Davis.** 1986. Coronavirus IBV: removal of spike glycopolypeptide S1 by urea abolishes infectivity and haemagglutination but not attachment to cells. J. Gen. Virol. **67**(Pt 7)**:**1443–1448.
17. **Cavanagh, D., et al.** 1986. Coronavirus IBV: partial amino terminal sequencing of spike polypeptide S2 identifies the sequence Arg-Arg-Phe-Arg-Arg at the cleavage site of the spike precursor propolypeptide of IBV strains Beaudette and M41. Virus Res. **4:**133–143.
18. **Chutinimitkul, S., et al.** 2010. *In vitro* assessment of attachment pattern and replication efficiency of H5N1 influenza A viruses with altered receptor specificity. J. Virol. **84:**6825–6833. doi:10.1128/JVI.02737-09.

19. **Colwell, W. M., and P. D. Lukert.** 1969. Effects of avian infectious bronchitis virus (IBV) on tracheal organ cultures. Avian Dis. **13:**888–894.

20. **Cornelissen, L. A., et al.** 2010. A single immunization with soluble recombinant trimeric hemagglutinin protects chickens against highly pathogenic avian influenza virus H5N1. PLoS One **5:**e10645. doi:10.1371/journal.pone.0010645.

21. **Delmas, B., and H. Laude.** 1990. Assembly of coronavirus spike protein into trimers and its role in epitope expression. J. Virol. **64:**5367–5375.

22. **de Vries, R. P., et al.** 2010. The influenza A virus hemagglutinin glycosylation state affects receptor-binding specificity. Virology **403:**17–25. doi:10.1016/j.virol.2010.03.047.

23. **de Vries, R. P., et al.** 20 December 2010. Only two residues are responsible for the dramatic difference in receptor binding between swine and new pandemic H1 hemagglutinin. J. Biol. Chem. doi:10.1074/jbc.M110.193557.

24. **Fang, S. G., S. Shen, F. P. Tay, and D. X. Liu.** 2005. Selection of and recombination between minor variants lead to the adaptation of an avian coronavirus to primate cells. Biochem. Biophys. Res. Commun. **336:**417–423.

25. **Gallardo, R. A., V. L. van Santen, and H. Toro.** 2010. Host intraspatial selection of infectious bronchitis virus populations. Avian Dis. **54:**807–813.

26. **Gambaryan, A., R. Webster, and M. Matrosovich.** 2002. Differences between influenza virus receptors on target cells of duck and chicken. Arch. Virol. **147:**1197–1208. doi:10.1007/s00705-002-0796-4.

27. **Gambaryan, A. S., et al.** 2004. H5N1 chicken influenza viruses display a high binding affinity for Neu5Acα2-3Galβ1–4(6-HSO3)GlcNAc-containing receptors. Virology **326:**310–316. doi:10.1016/j.virol.2004.06.002.

28. **Geilhausen, H. E., F. B. Ligon, and P. D. Lukert.** 1973. The pathogenesis of virulent and avirulent avian infectious bronchitis virus. Arch. Gesamte Virusforsch. **40:**285–290.

29. **Godet, M., J. Grosclaude, B. Delmas, and H. Laude.** 1994. Major receptor-binding and neutralization determinants are located within the same domain of the transmissible gastroenteritis virus (coronavirus) spike protein. J. Virol. **68:**8008–8016.

30. **Guo, C. T., et al.** 2007. The quail and chicken intestine have sialyl-galactose sugar chains responsible for the binding of influenza A viruses to human type receptors. Glycobiology **17:**713–724. doi:10.1093/glycob/cwm038.

31. **Haijema, B. J., H. Volders, and P. J. Rottier.** 2003. Switching species tropism: an effective way to manipulate the feline coronavirus genome. J. Virol. **77:**4528–4538.

32. **Harbury, P. B., T. Zhang, P. S. Kim, and T. Alber.** 1993. A switch between two-, three-, and four-stranded coiled coils in GCN4 leucine zipper mutants. Science **262:**1401–1407.

33. **Hodgson, T., R. Casais, B. Dove, P. Britton, and D. Cavanagh.** 2004. Recombinant infectious bronchitis coronavirus Beaudette with the spike protein gene of the pathogenic M41 strain remains attenuated but induces protective immunity. J. Virol. **78:**13804–13811.

34. **Hopkins, S. R., and H. W. Yoder, Jr.** 1986. Reversion to virulence of chicken-passaged infectious bronchitis vaccine virus. Avian Dis. **30:**221–223.

35. **Ignjatovic, J., and L. Galli.** 1994. The S1 glycoprotein but not the N or M proteins of avian infectious bronchitis virus induces protection in vaccinated chickens. Arch. Virol. **138:**117–134.

36. **Jackwood, M. W., et al.** 2001. Spike glycoprotein cleavage recognition site analysis of infectious bronchitis virus. Avian Dis. **45:**366–372.

37. **Johnson, M. A., C. Pooley, J. Ignjatovic, and S. G. Tyack.** 2003. A recombinant fowl adenovirus expressing the S1 gene of infectious bronchitis virus protects against challenge with infectious bronchitis virus. Vaccine **21:**2730–2736.

38. **Koch, G., L. Hartog, A. Kant, and D. J. van Roozelaar.** 1990. Antigenic domains on the peplomer protein of avian infectious bronchitis virus: correlation with biological functions. J. Gen. Virol. **71**(Pt 9)**:**1929–1935.

39. **Koch, G., and A. Kant.** 1990. Binding of antibodies that strongly neutralise infectious bronchitis virus is dependent on the glycosylation of the viral peplomer protein. Adv. Exp. Med. Biol. **276:**143–150.

40. **Krempl, C., H. Laude, and G. Herrler.** 1998. Is the sialic acid binding activity of the S protein involved in the enteropathogenicity of transmissible gastroenteritis virus? Adv. Exp. Med. Biol. **440:**557–561.

41. **Krempl, C., B. Schultze, H. Laude, and G. Herrler.** 1997. Point mutations in the S protein connect the sialic acid binding activity with the enteropathogenicity of transmissible gastroenteritis coronavirus. J. Virol. **71:**3285–3287.

42. **Kuo, L., G. J. Godeke, M. J. Raamsman, P. S. Masters, and P. J. Rottier.** 2000. Retargeting of coronavirus by substitution of the spike glycoprotein ectodomain: crossing the host cell species barrier. J. Virol. **74:**1393–1406.

43. **Laude, H., et al.** 1995. Functional domains in the spike protein of transmissible gastroenteritis virus. Adv. Exp. Med. Biol. **380:**299–304.

44. **Lin, X. Q., V. N. Chouljenko, K. G. Kousoulas, and J. Storz.** 2000. Temperature-sensitive acetylesterase activity of haemagglutinin-esterase specified by respiratory bovine coronaviruses. J. Med. Microbiol. **49:**1119–1127.

45. **Liu, S., et al.** 2009. Altered pathogenicity, immunogenicity, tissue tropism and 3′-7kb region sequence of an avian infectious bronchitis coronavirus strain after serial passage in embryos. Vaccine **27:**4630–4640.

46. **Madu, I. G., et al.** 2007. Heparan sulfate is a selective attachment factor for the avian coronavirus infectious bronchitis virus Beaudette. Avian Dis. **51:**45–51.

47. **McKinley, E. T., D. A. Hilt, and M. W. Jackwood.** 2008. Avian coronavirus infectious bronchitis attenuated live vaccines undergo selection of subpopulations and mutations following vaccination. Vaccine **26:**1274–1284.

48. **Meulemans, G., et al.** 2001. Epidemiology of infectious bronchitis virus in Belgian broilers: a retrospective study, 1986 to 1995. Avian Pathol. **30:**411–421.

49. **Nicholls, J. M., A. J. Bourne, H. Chen, Y. Guan, and J. S. Peiris.** 2007. Sialic acid receptor detection in the human respiratory tract: evidence for widespread distribution of potential binding sites for human and avian influenza viruses. Respir. Res. **8:**73. doi:10.1186/1465-9921-8-73.

50. **Otsuki, K., K. Noro, H. Yamamoto, and M. Tsubokura.** 1979. Studies on avian infectious bronchitis virus (IBV). II. Propagation of IBV in several cultured cells. Arch. Virol. **60:**115–122.

51. **Pensaert, M., and C. Lambrechts.** 1994. Vaccination of chickens against a Belgian nephropathogenic strain of infectious bronchitis virus B1648 using attenuated homologous and heterologous strains. Avian Pathol. **23:**631–641. doi:10.1080/03079459408419033.

52. **Pohlmeyer, I., et al.** 2005. Lectin histochemical investigations of the distal gut of chicks with special emphasis on the follicle-associated epithelium. J. Vet. Med. A Physiol. Pathol. Clin. Med. **52:**138–146. doi:10.1111/j.1439-0442.2005.00696.x.

53. **Raj, G. D., and R. C. Jones.** 1997. Infectious bronchitis virus: immunopathogenesis of infection in the chicken. Avian Pathol. **26:**677–706.

54. **Sanchez, C. M., et al.** 1999. Targeted recombination demonstrates that the spike gene of transmissible gastroenteritis coronavirus is a determinant of its enteric tropism and virulence. J. Virol. **73:**7607–7618.

55. **Schultze, B., D. Cavanagh, and G. Herrler.** 1992. Neuraminidase treatment of avian infectious bronchitis coronavirus reveals a hemagglutinating activity that is dependent on sialic acid-containing receptors on erythrocytes. Virology **189:**792–794.

56. **Schultze, B., et al.** 1996. Transmissible gastroenteritis coronavirus, but not the related porcine respiratory coronavirus, has a sialic acid (*N*-glycolylneuraminic acid) binding activity. J. Virol. **70:**5634–5637.

57. **Schwegmann-Wessels, C., and G. Herrler.** 2006. Sialic acids as receptor determinants for coronaviruses. Glycoconj. J. **23:**51–58. doi:10.1007/s10719-006-5437-9.

58. **Siddell, S. G. (ed.).** 1995. The *Coronaviridae*. Plenum Press, New York, NY.

59. **Song, C. S., et al.** 1998. Induction of protective immunity in chickens vaccinated with infectious bronchitis virus S1 glycoprotein expressed by a recombinant baculovirus. J. Gen. Virol. **79**(Pt 4)**:**719–723.

60. **Spaan, W., D. Cavanagh, and M. C. Horzinek.** 1988. Coronaviruses: structure and genome expression. J. Gen. Virol. **69**(Pt 12)**:**2939–2952.

61. **Sriwilaijaroen, N., et al.** 2009. Analysis of N-glycans in embryonated chicken egg chorioallantoic and amniotic cells responsible for binding and adaptation of human and avian influenza viruses. Glycoconj. J. **26:**433–443. doi:10.1007/s10719-008-9193-x.

62. **Stevens, J., et al.** 2006. Glycan microarray analysis of the hemagglutinins from modern and pandemic influenza viruses reveals different receptor specificities. J. Mol. Biol. **355:**1143–1155. doi:10.1016/j.jmb.2005.11.002.

63. **Stevens, J., O. Blixt, J. C. Paulson, and I. A. Wilson.** 2006. Glycan microarray technologies: tools to survey host specificity of influenza viruses. Nat. Rev. Microbiol. **4:**857–864.

64. **Stevens, J., et al.** 2006. Structure and receptor specificity of the hemagglutinin from an H5N1 influenza virus. Science **312:**404–410. doi:10.1126/science.1124513.

65. **Taguchi, F.** 1995. The S2 subunit of the murine coronavirus spike protein is not involved in receptor binding. J. Virol. **69:**7260–7263.

66. **Tumpey, T. M., et al.** 2007. A two-amino acid change in the hemagglutinin of the 1918 influenza virus abolishes transmission. Science **315:**655–659.

67. **van Santen, V. L., and H. Toro.** 2008. Rapid selection in chickens of subpopulations within ArkDPI-derived infectious bronchitis virus vaccines. Avian Pathol. **37:**293–306. doi:10.1080/03079450802043783.

68. **Winter, C., G. Herrler, and U. Neumann.** 2008. Infection of the tracheal epithelium by infectious bronchitis virus is sialic acid dependent. Microbes Infect. **10:**367–373.

69. **Winter, C., C. Schwegmann-Wessels, D. Cavanagh, U. Neumann, and G. Herrler.** 2006. Sialic acid is a receptor determinant for infection of cells by avian infectious bronchitis virus. J. Gen. Virol. **87:**1209–1216.

70. **Wong, S. K., W. Li, M. J. Moore, H. Choe, and M. Farzan.** 2004. A 193-amino acid fragment of the SARS coronavirus S protein efficiently binds angiotensin-converting enzyme 2. J. Biol. Chem. **279:**3197–3201. doi:10.1074/jbc.C300520200.

71. **Yamada, Y., and D. X. Liu.** 2009. Proteolytic activation of the spike protein at a novel RRRR/S motif is implicated in furin-dependent entry, syncytium formation, and infectivity of coronavirus infectious bronchitis virus in cultured cells. J. Virol. **83:**8744–8758.

72. **Yokomori, K., et al.** 1995. Neuropathogenicity of mouse hepatitis virus JHM isolates differing in hemagglutinin-esterase protein expression. J. Neurovirol. **1:**330–339.

73. **Zeng, Q., M. A. Langereis, A. L. van Vliet, E. G. Huizinga, and R. J. de Groot.** 2008. Structure of coronavirus hemagglutinin-esterase offers insight into corona and influenza virus evolution. Proc. Natl. Acad. Sci. U. S. A. **105:**9065–9069. doi:10.1073/pnas.0800502105.